P6.17 INTERCOMPARISON AND DIAGNOSIS OF MEI-YU RAINFALL DERIVED FROM SATELLITE DATA

Y. Zhou *
Department of Meteorology, University of Maryland, College Park, Maryland
P. A. Arkin
ESSIC, University of Maryland, College Park, Maryland

1. Introduction

Monsoons are driven by seasonal winds caused primarily by the greater annual variation in air temperature over large land surfaces compared to ocean surfaces. During the early summer in East Asia, dry cold air from the Eurasian continent and warm moist air from the West Pacific converge and form a frontal zone.

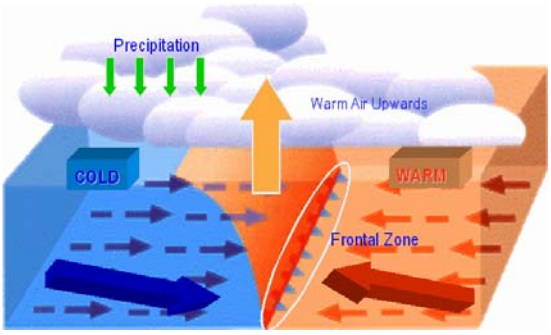

Fig.1. Cold air and warm air meet each other and form the frontal zone at convergence area; lighter warm air goes upward which is known as convection and precipitation will occur near the frontal zone line; when cold air and warm air is comparable to each other, frontal zone will be steady for a period of time thus cause a continuous rainy period. (Based on the cartoon adapted from http://earth.fg.tp.edu.tw/learn/esf/magazine/980302.htm, Chen, 1998, *Journal of Earth Science, Taiwan,* **5**)

* *Corresponding author address:* Yan Zhou, Univ. of Maryland, Dept. of Meteorology, College Park, MD 20742; E-mail: katjo@atmos.umd.edu

The frontal zone results in a zonally-oriented rain belt, located on the northwestern edge of the West Pacific high. The Chinese term Mei-Yu (which means *plum rain*) refers to a continuous regional rainy season specifically over the Yangtze River Valley in East China, which is initiated by the planetary-scale rainband advancing across East Asia continent during the East Asia summer monsoon period. The same rainy season over Japan is called Baiu while in Korea is called Mae-ue.

The Mei-Yu season brings the most important extended rainfall in the East Asian region. More than 1000mm of rainfall is observed during Baiu period in Japan. In the Yangtze River Valley, about 25% of the rainfall of whole year is obtained during the Mei-Yu period, which is only about 3 to 7 weeks. In some heavy Mei-Yu seasons, the percentage is over 40%. The Yangtze River Valley is one of the most important regions of population, agriculture and economics in China. Annual and interannual variations of Mei-Yu rainfall induce severe floods of the Yangtze River and drought events over the region. An improved description and understanding of the characteristics of Mei-Yu rainfall is necessary to improve predictions of this phenomenon.

2. Data

In this study we use several different estimates of large-scale precipitation, mainly based on satellite data but in some cases including gauge observations, to examine the annual and interannual variation of precipitation over the Mei-Yu region (110°~125°E, 25°~35° N). We will utilize two composite datasets: the CMAP (CPC Merged Analysis of Precipitation – Xie and Arkin, 1997) and GPCPv2 (Global Precipitation Climatology Project Version 2 – Huffman, Bolvin and Adler, 2003). These composite datasets combine several estimates based on satellite observations with observations from rain gauges. We will also examine precipitation estimates based only on satellite observations, including TOVS (TIROS Operational Vertical Sounder) based on NOAA polar orbiting satellite observations (Susskind et al., 1989), GPI (GOES Precipitation Index) from geostationary satellite infrared data (Arkin and Meisner, 1997), OPI (OLR Precipitation Index) from NOAA AVHRR data (Xie and

Table 1. Satellite, gauge and composite datasets used in this work.

Data Sets	Satellite	Technique	Algorithm	Time Period	Grid
Satellite					
SSM/I Scattering	Polar-Orbiting	Passive Microwave	Ice Particles	07/1987 – P	2.5°x2.5°
TOVS	Polar-Orbiting	IR	Clouds Volume	01/1987 – P	
OPI	Geostationary	ORL	Clouds Tops	01/1979 – P	
GPI	Geostationary	IR	Clouds Tops	01/1986 – P	
AGPI	Geostationary	IR+Microwave	Merged GPI+ SSM/I/TOVS	01/1986 – P	
Merged					
CMAP	GHCN+CAMS[1] (Rain Gauge); GPCC[2] (Rain Gauge); GPI, OPI; SSM/I scattering; SSM/I emission; MSU[3]; Atolls.			01/1979 – P	2.5°x2.5°
GPCP	GHCN+CAMS[1] (Rain Gauge); GPCC[2] (Rain Gauge); GPI, OPI; TOVS; SSM/I scattering; SSM/I emission; SSM/I composite; SSM/I/TOVS composite; AGPI; Multi-Satellite; Satellite Gauge.			01/1979 – P	
Gauge					
PREC	Optimum Interpolation of gauge observations at over 17,000 stations collected in the NOAA/NCDC GHCN Version 2 and the NOAA/CPC CAMS data sets.			01/1948 – P	2.5°x2.5°

1, Global Historical Climatology Network (GHCN) of NOAA/NCDC and the Climate Anomaly Monitoring System (CAMS) of NOAA/CPC;

2, Global Precipitation Climatology Center (GPCC) for the Global Precipitation Center Project (GPCP), initiated under the World Climate Research Program;

3, the Microwave Sounding Unit (MSU) is on board NOAA's TIROS-N polar-orbiting satellite in October of 1978.

Arkin, 1998), estimates based on passive microwave data from SSM/I (Special Sensor Microwave/Imager) scattering (Ferraro et al., 1997) and AGPI (Adjusted GPI) which is GPI adjusted by combination with merged SSM/I/TOVS precipitation (Huffman et al., 1997). The datasets to be used have different characteristics, cover different time periods, and have different spatial and temporal resolutions.

3. Mean Annual Cycle

Mei-Yu is the label for the spring rainy season over the Yangtze River Valley in East China. In this study we chose a region comprising 6 2.5°x2.5° grid boxes covering the area from 111.25°~118.75°E and 28.75°~33.75°N (see box outlined in figure 2). This is the region along the lower Yangtze River and extending to the north to the Huaihe River region.

Figure 2 presents the monthly average precipitation rates over East China from GPCP for May - August. In May, the distribution of monthly precipitation rate has a pronounced zonally-oriented pattern. The maximum of precipitation is along a zonal belt, primarily located in South China.

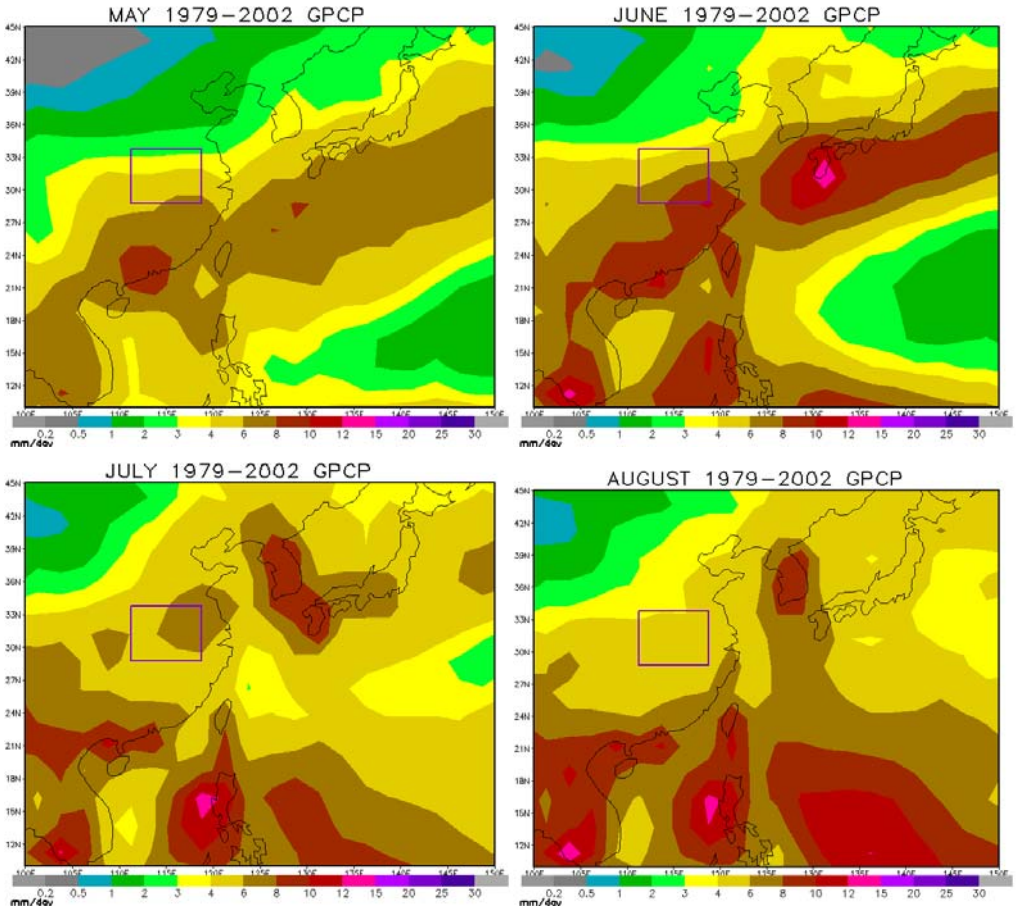

Fig.2. Monthly average precipitation rate (*mm/day*) in East Asia area. Mei-Yu region is the area within around *110°E and east, 27°~34°N*. Box in the plots, *111.25°~118.75°E, 28.75°~33.75°N*.

There is a clear minimum precipitation area over the ocean associated with the west Pacific high. In June, the rain belt moves northwards extended from Southeast China to South Japan. The maximum value along the rain belt increases. The Mei-Yu season begins with this progression. The minimum precipitation area over the ocean also moves northwards and becomes bigger. In July, the rain belt appears to fragment. However, the maximum value again moves northward to the Yellow River area of northern China. The rainy season of northern China begins, while over the Yangtze River Valley the Mei-Yu rainy season is usually over in this month. The minimum value above the ocean also retreats to the west. In August, no maximum value is seen over China; on this monthly time scale, the zonally-oriented structure appears to fade away without any clear southward migration.

According to M.M.Yoshino (1971), the Mei-Yu season consists of four stages. In the middle of May, the front associated with heavy rainfall extends from the southern coast of China into the western Pacific. The rain belt strengthens and elongates and moves northwards in June to the Yangtze River Valley in China, where it produces the original Mei-Yu (Plum rain). Then the rain belt continues to move northward to northern China, leading to a heavy rainy season in northern China in July and August. It then begins to weaken and withdraw southward again. The evolving precipitation pattern in figure 2 corresponds to this classic pattern in many respects, but not all. For example, we do not see a clear sign of an orderly southward progression at the end of the season. This may be due to our use of the monthly time scale.

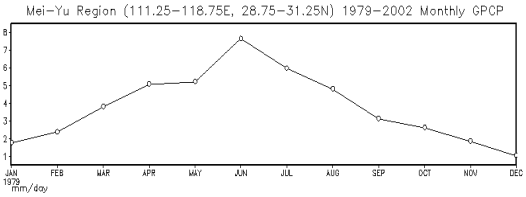

Fig.3. 24-year average monthly precipitation rate from GPCP *(111.25°~118.75°E, 28.75°~31.25°N).*

Figure 3 displays the annual cycle of precipitation within the Mei-Yu region along the Yangtze River Valley (111.25°~118.75°E, 28.75°~31.25°N). Precipitation rate in the figure is taken from the 24-year average of GPCP monthly precipitation for the period 1979 – 2002. It shows clearly that summer is the rainy season in this area. In June when the Mei-Yu season peaks in this area, the monthly precipitation rate is at least 1.5 mm/day larger than any other month. Furthermore, the change from May to June is the largest month-to-month change found in this region.

Figure 4 presents the time series of GPCP monthly precipitation over the Mei-Yu region. Floods and severe floods recorded in 1980, 1983, 1991, 1996 and 1998 can be clearly seen in this plot. Severe drought events in 1988, 1994 and 2001 also can be seen in the interannual variability for each every month over the Mei-Yu region (fig. 5). Large anomalies can be seen throughout the year, since, as seen in figure 4, precipitation occurs in this region in all seasons. However, only during the Mei-Yu season is there sufficient precipitation on the average that large anomalies often lead to significant flood events in the region.

4. Intercomparison between Datasets

The GPCP precipitation is based on a combination of several satellite-derived estimates as well as gauge data. One of its

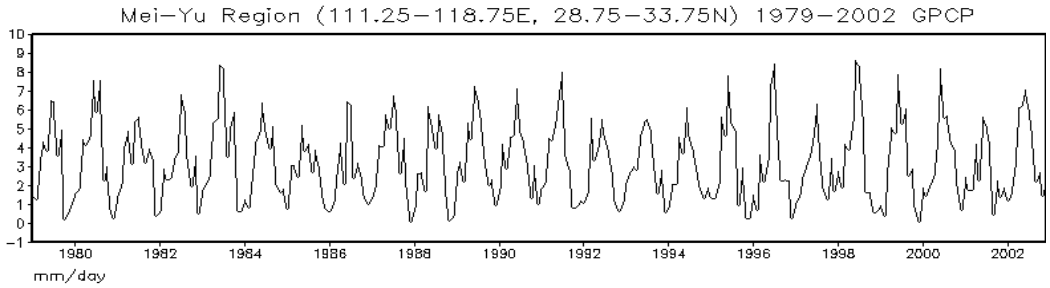

Fig. 4. Time series of monthly average precipitation from GPCP *(111.25°~118.75°E, 28.75°~33.75°N)*.

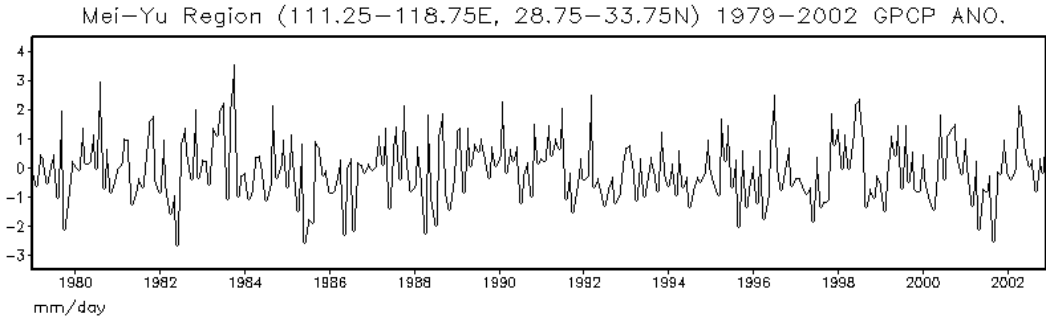

Fig. 5. Time series of monthly precipitation anomaly from GPCP *(111.25°~118.75°E, 28.75°~33.75°N)*.

components is the AGPI, which is GPI adjusted with combined SSM/I/TOVS. Both emission and scattering estimates derived from SSM/I are used in GPCP, the former over the oceans and the latter over land. Emission estimates are based on lower frequency radiances, and are based on the emission from raindrops. Such estimates are feasible only over the ocean since the land surface emissivity is very complex. Over land surface, estimates are derived from higher frequency radiances, where large ice particles associated with convective precipitation scatters upwelling surface radiation and reduces the apparent radiating temperature. The scattering estimates used in this study are from Ferraro (1997). There are two satellites, both in sun-synchronous orbits, one with an equator crossing time of 6 am and 6 pm, and the other at 10 am and 10 pm. Estimates are derived separately and then merged with weighting by the number of samples in every month.

Figure 6 shows time series of precipitation over the Mei-Yu region derived from various data sets. GPCP and CMAP merged data exhibit variability very similar to PREC, which is based entirely on rain gauge data. This is due to the strong influence of the gauge observations on both GPCP and CMAP over land. The other IR-based estimates, OPI, GPI and AGPI, agree in general with GPCP and CMAP, but with some differences in details.

Figure 7 shows the 10-year averaged monthly mean precipitation pattern for May for the various data sets. CMAP and GPCP agree well in the Mei-Yu region, presumably because they are both based on merged multiple satellite-derived estimates and rain gauge data. The gauge data balance the bias from satellite observation. The difference between GPCP and the gauge-based PREC is negative in the Mei-

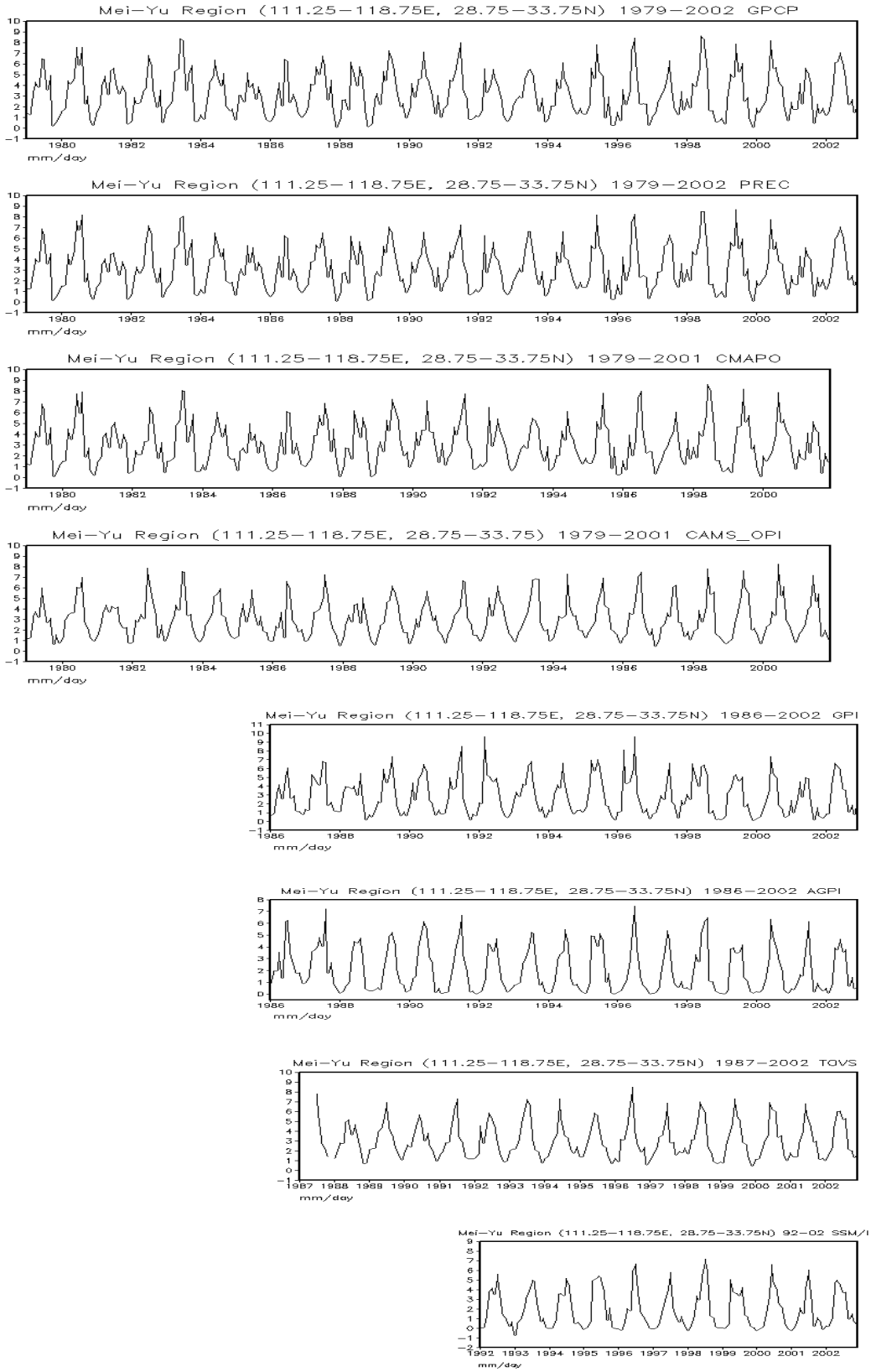

Fig. 6. Time series of monthly precipitation from various datasets *(111.25°~118.75°E, 28.75°~33.75°N)*.

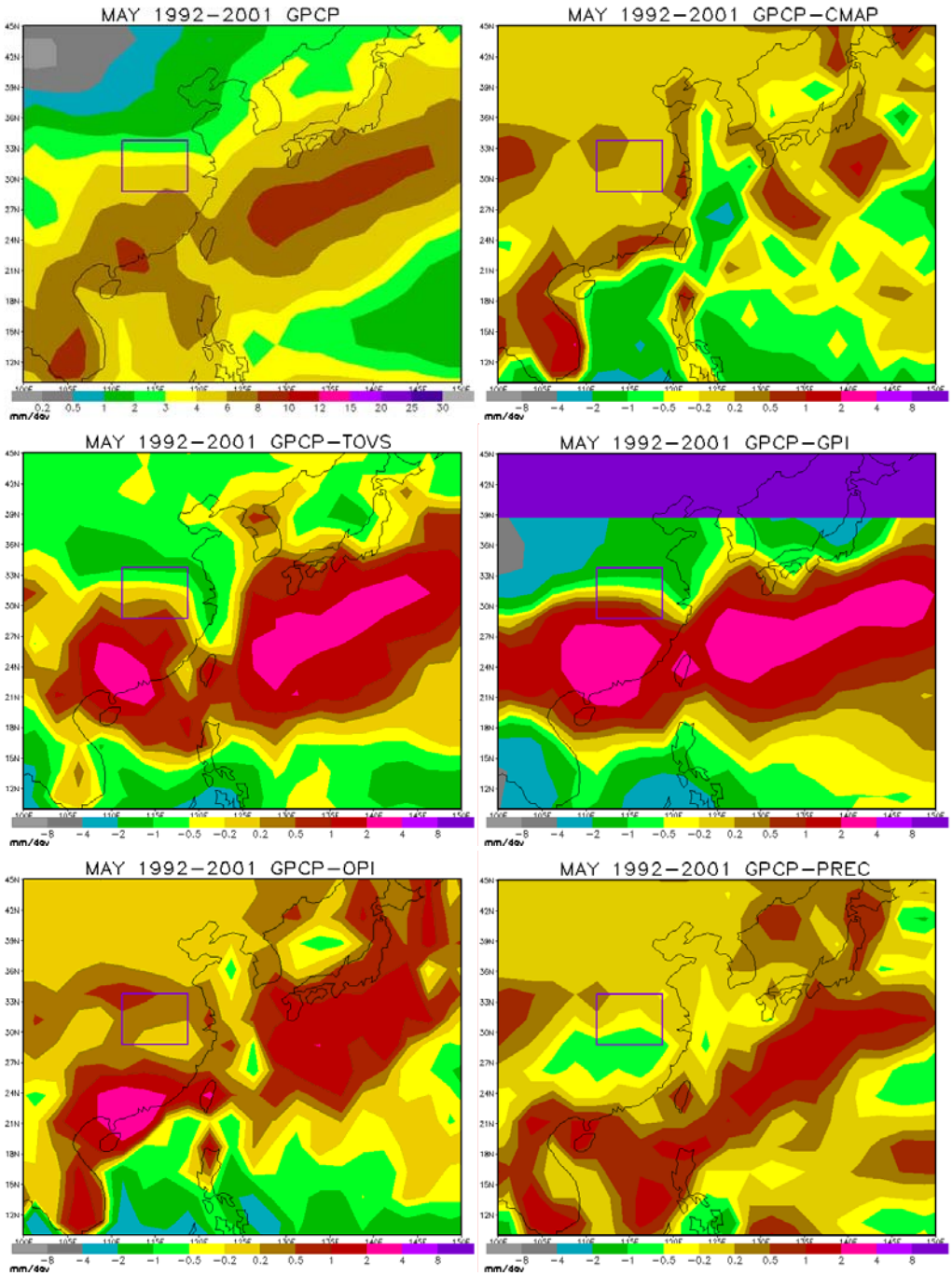

Fig. 7. Intercomparison of the 10-year (from 1992 to 2001) mean precipitation pattern for May. Box in the plots, *111.25°~118.75°E, 28.75°~33.75°N*.

-Yu region, while the difference between GPCP and most of the satellite estimates is positive in that region, possibly indicating that satellite data tend to relatively underestimate the precipitation rate in the Mei-Yu region. The time period we chose for our comparison of other data sets with GPCP is the 10 years from 1992 to 2001. Among the satellite-based estimates, OPI has the best agreement with the merged data sets over the Mei-Yu region and land in general, probably because OPI uses gauge observations in its calibration. GPI and

TOVS provide similar descriptions of large-scale variability over both land and ocean in May and June, which is reasonable since both are derived from satellite infrared observations of cloudiness. However, in July and August (not shown) following the Mei-Yu period, their patterns are different.

5. Conclusions and Further Work

In this study, the characteristics of Mei-Yu rainfall has been described using several data sets based on a variety of in situ and satellite observations. The sensitivity of features such as annual and interannual variations has been examined.

The features of Mei-Yu rainfall found in this study are consistent with previous work. However, some features, such as a clear sign of an orderly southward progression at the end of the season, are not seen here. This may be due to our use of the monthly time scale. In further work we will utilize pentad data to examine the more detailed characteristics and evolution of Mei-Yu precipitation. By intercomparing the results derived from different data sets, we found some differences in the satellite-derived precipitation estimates. Compared with rain gauge derived results, satellite observations tend to underestimate the precipitation rate in the early stage of Mei-Yu. However, the withdrawal stage of the Mei-Yu appears to have a different pattern of difference, which will be examined in our future work.

REFERENCE

Chang, C.-P., Zhang, Yongsheng, and Li, Tim, 1999: Interannual and Interdecadal Variations of the East Asian Summer Monsoon and Tropical Pacific SSTs. Part I: Roles of the Subtropical Ridge. *Journal of Climate,* Vol. 13.

Ferraro, Ralph R., 1997: Special Sensor Microwave Imager Derived Global Rainfall Estimates for Climatological Applications, *Journal of Geophysical Research, Vol. 102, No.D14, 16,715-16,735,*.

Janowiak, John E. and Xie, PingPing, 2003: A Global-Scale Examination of Monsoon-Related Precipitation, *Journal of Climate,* Vol.16.

Lau, K.-M. and Yang, Song, 1996: Climatology and Interannual Variability of the Southeast Asian Summer Monsoon. *Submitted to Advances in Atmospheric Sciences*.

McCollum, Jeffrey R. and Ferraro, Ralph R., 2003: Next Generation of NOAA/NESDIS TMI, SSM/I, and AMSR-E Microwave Land Rainfall Algorithms, *Journal of Geophysical Research,* Vol. 108, No.D8, 3882.

McCollum, Jeffrey R., Krajewski, Witold F., Ferraro, Ralph R., and Ba, Mamoudou B., 2002: Evaluation of Biases of Satellite Rainfall Estimation Algorithms over the Continental United States, *Journal of Applied Meteorology,* Vol.41.

Qian, W. and Yang, S., 2000: Onset of the Regional Monsoon Over Southeast Asia, *Meteorology and Atmospheric Physics,* **75**, 29-38.

Rodwell, M.J. and Hoskins, B. J., 2000: Subtropical Anticyclones and Summer Monsoons, *Journal of Climate,* Vol. 14.

Wang, B., LinHo, Y. Zhang, M.-M. Lu, 2002: A Unified Definition of the Summer Monsoon Onset over the South China Sea and East Asia, *Submitted to Journal of Climate*.

Xie, Pingping, Janowiak, John E., Arkin, Phillip A., 2003: Robert Adler, Arnold Gruber, Ralph Ferraro, George J. Huffman, and Scott Curtis, GPCP Pentad Precipitation Analyses: An Experimental Dataset Based on Gauge Observations and Satellite Estimates. *Journal of Climate,* Vol. 16.

Yin, Xungang, Gruber, Arnold, and Arkin, Phillip A., 2004: Comparison of the GPCP and CMAP Merged Gauge-satellite Monthly Precipitation Products for the Period 1979-2001, *Submitted to JHM*.

Yoshino, M. M., 1971: Water Balance Of Monsoon Asia, *University of Hawaii Press*.